JOURNAL OF NANO- AND ELECTRONIC PHYSICS
Vol. **5** No 3, 03001(4pp) (2013)

ЖУРНАЛ НАНО- ТА ЕЛЕКТРОННОЇ ФІЗИКИ
Том **5** № 3, 03001(4cc) (2013)

Characterization of Coated Fe-Doped Zinc Oxide Nanostructures

M. Benhaliliba[1,*], Y.S. Ocak[2], A. Tab[1]

[1] *Physics Department, Science Faculty, Oran University of Sciences and Technology USTO-MB, BP1505 Oran, Algeria*
[2] *Department of Science, Faculty of Education, University of Dicle, Diyarbakir, Turkey*

(Received 23 December 2012; revised manuscript received 01 July 2013; published online 15 July 2013)

The nanostructures of iron-doped zinc oxide (FZO) produced by a simple and low cost dip-coating route onto a glass substrate were studied. The structural, morphological, electrical and optical properties of FZO films were investigated. Nanochains were revealed by SEM analysis at high magnification. A (002)-oriented wurzite structure with a lattice parameter of $a = 3.24$ Å and $c = 5.19$ Å was confirmed by X-rays diffraction. High transmittance was exhibited in the visible spectrum, T (550 nm) > 83 %. Finally, electrical measurements revealed a resistivity and mobility of 10 kΩ·cm, and 5 cm² / Vs respectively.

Keywords: Nanostructures, ZnO films, Fe-doping, Dip coating, X-rays pattern, SEM, Resistivity.

PACS number: 75.50 Pp

1. INTRODUCTION

Zinc oxide (ZnO) films have been among the most investigated oxides in recent years, principally due to its applications in opto-electronic devices [1-2]. In order to further to explore properties and applications of ZnO, known as multifunctional material, many additive metallic elements have been used to dope ZnO, such as Al, In, Cu, Sn and Fe[2-6]. Up to date, few works on iron doped zinc oxide (FZO) produced by dip coating were achieved. In the present work, we produced coated FZO films by a facile and low cost dip coating route. Physical and surface analyses of the coated films were investigated and the role of iron on crystalline structure and surface morphology of ZnO films was emphasized.

2. EXPERIMENTAL DETAILS

ZnO was produced through a facile sol-gel dip coating route. 0.4 M of zinc acetate ($Zn(CH_3COO)_2.2(H_2O)$) (99 %, Riedel-de Haer) was used as starting material and iron (III) chloride hexahydrate ($FeCl_3.6(H_2O)$) as doping precursor. Fe/Zn ratio was taken equal to 2 and 3 % in the solution. Both precursor and doping source have been dissolved in ethanol (96 %, Riedel-de Haer), stirred at 70 °C for 10 min. Firstly, substrates were cleaned in ultrasonic bath at 35 °C. The substrates were washed by ethanol, acetone and distilled water during 20 min, then dried by nitrogen gas. The substrate was dipped in the prepared solution and heated at 120 °C; the process of diping was regularly repeated ten times. The obtained film was then annealed at 400 °C for 300 min. XRD analysis of samples was carried out using Rigaku Mini-flex XRD system equipped with CuK_α radiation of average wavelength of 1.54 Å, supplied by 30 kV / 15 mA, measurements were done in the peak regions 0.01-0.05 angle intervals 2 theta/theta mode. JOEL JSM 7001F SEM was used to analyze the surface morphology of the samples. Optical spectroscopy was carried out using UV-VIS spectrophotometer Perkin Elmer lambda 25. Electrical measurements were performed by the means of ECOPIA HMS 3000 Hall Effect measurement system at room temperature using a magnetic field of 0.58 T.

3. RESULTS AND DISCUSSION

3.1 Structural and Surface Studies

Fig. 1 depicts the X-rays patterns of 2 and 3 % doped ZnO in the range of 20°-80°. An angle shift, $\Delta(2\theta)$ equal to 0.03° and 0.20° for 2 % and 3 % doped ZnO respectively was observed. The films exhibited polycrystalline structure with two important directions that were (002) and (101). Indeed, these reflections peaked at 34.45° and 34.62° respectively, identified the wurtzite structure of our as-grown films. Table 1 summarized all parameters of the X-rays analysis. Based on JCPDS card No 36-1451 of pure ZnO, the X-rays patterns confirmed the presence of the ZnO wurtzite phase [2], but a peak, labeled with a star in Fig. 1, positioned at 42.8° doesn't belong to the ZnO phase. It may identify the iron oxide phase. The grain size G, determined by the well-known Scherrer formula, decreased from 35 nm to 25 nm with an increase in iron content in the solution as listed below. The lattice parameters a and c were found to be around 3.2 Å and 5.1 Å respectively, the obtained values of lattice parameters 3.25 Å and 5.20 Å were reported by Carvalho [7]. The SEM images showed a homogenous surface of Fe-doped ZnO films as displayed in Fig. 2. The assembled nanospheres of Fe doped ZnO were observed by high magnification SEM analysis. These latter were so bound that built structures looking like nanochains as shown in SEM pictures (Fig. 2a, b, c, d). The nanochains have grown in different directions leaving micro-voids in the surface. The nanochains are straight, and have a bright appearance, and composed a lattice in the majority of the surface with apparent boundaries as shown in Fig. 2c and d. Roughly, the chains have lengths within the range of 50-300 nm.

* mbenhaliliba@gmail.com

 © 2013 Sumy State University

Table 1 – The (hkl) planes, Bragg angle, d-spacing, angle shift, Grain size, Intensity of peaks, lattice parameters

Fe-Doping level (%)	(hkl) Planes	2θ (deg.)	d_{hkl} (Å)	$\Delta(2\theta)$ (deg.)	G (nm)	I (a.u)	c (Å)	a (Å)	c/a
2	(002)	34.45	2.594	0.03	35.520	100.83	5.19	3.24	1.601
	(101)	36.35	2.469	0.40	–	58.10			
3	(002)	34.62	2.574	0.20	25.041	154.60	5.15	3.26	1.578
	(101)	36.23	2.477	0.02	–	64.20			

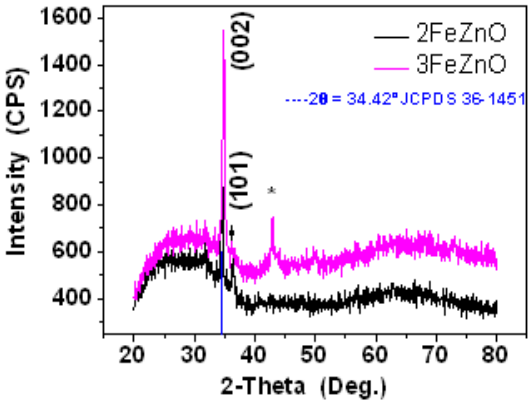

Fig. 1 – X-rays pattern of coated AZO film within the range of angle 20-80 degrees. Slight shift of (002) peak as shown inset of figure, blue line located the peak (002) of JCPDS 36-1451 card

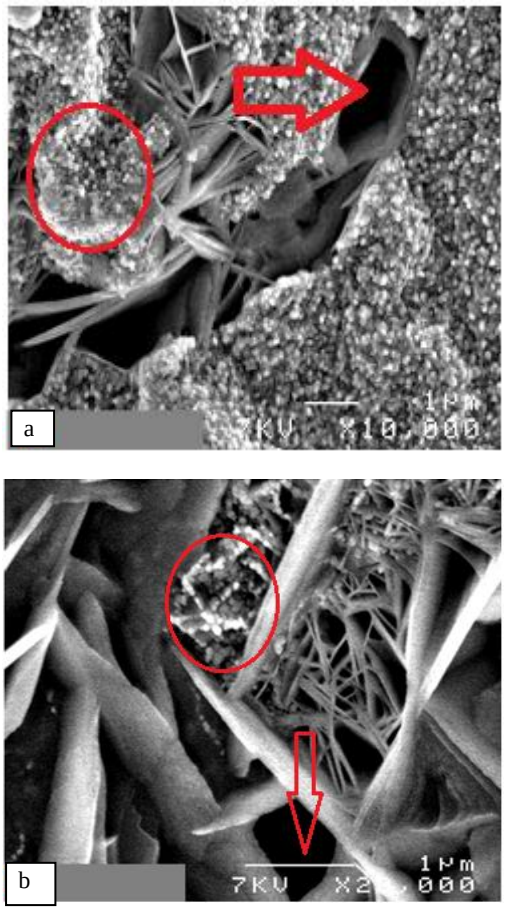

Fig. 2 – High magnification SEM pictures of Fe-doped ZnO nanostructures produced by dip- coating route, (a: × 10000), (b: × 20000) (c: × 30000) (d: × 50000). Nanochains were signed by red arrows and circles. Microvoids were indicated by arrow (Fig. a and b). A solid white bar showed a scale of 1 μm and 100 nm, voltage of SEM analysis was 7 kV. Bright nano-spheres and nanochains sizes were displayed in picture (d)

3.2 UV-VIS-IR Measurements

The UV-VIS-NIR transmittance of the as-grown 2 and 3 % Fe-doped ZnO films displayed as function of wavelength in the Fig. 3a. It is revealed that the transmittance of both 2 and 3 % Fe doped ZnO increases rapidly to a peak of 76 % in UV and VIS bands. A discrepancy between the two curves was clearly observed up to 900 nm due to difference in iron content in the solution. The optical band gap was determined by absorption plot and expressed by the formula 1 for the allowed direct transition [2]. The extrapolation intercepting the photon energy axis gives the optical band gap E_g as shown in Fig. 3b. It was found to be 3.24 eV and 3.26 eV for 2 and 3 % Fe-ZnO films respectively as listed in Table 2.

$$(\alpha h\nu)^2 = h\nu - E_g \quad (1)$$

A transmittance less than 85 % for Fe-doped ZnO has been reported by Xue et al. [8].

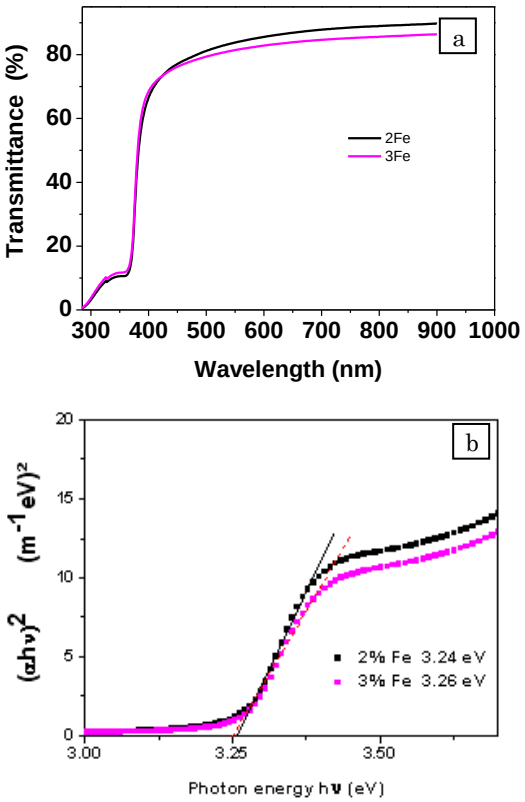

Fig. 3 – Sketch of transmittance versus photon wavelength of coated Fe-doped ZnO film (a). Variation of $(\alpha h\nu)^2$ against photon energy for the Fe-doped ZnO film (b)

3.3 Electrical Measurement

The sample was held between four gold contacts M, N, P and Q as sketched in Fig. 4. DC current of 1 nA was applied through the sample; a magnetic field, of 0.58 T, was applied perpendicular to sample as shown in Fig. 4. The Fe-doped ZnO films, grown by dip coating process, exhibited *p*-type conductivity. The electrical resistivity of as-grown films was calculated by [9],

$$\rho = \frac{VA}{lI} \quad (2)$$

where, V is the measured potential drop across the sample, I is the current through the sample, A is a cross section area through which the current runs and l is the separation of voltage leads. The films exhibited a resistivity in order of ten kilo Ohms, the mobility increased with a decrease in iron content.

The obtained charge carrier concentration was of $10^{13}\,\mathrm{cm}^{-3}$ for both 2 and 3 % Fe-doped ZnO films. The as-grown ZnO film exhibited n-type conductivity as cited previously [1-3]. It is revealed that iron ions could subsitute zinc sites and convert the n-type conductivity of zinc oxide to *p*-type. Resistive Fe-doped ZnO was also obtained by Colak et al. [10].

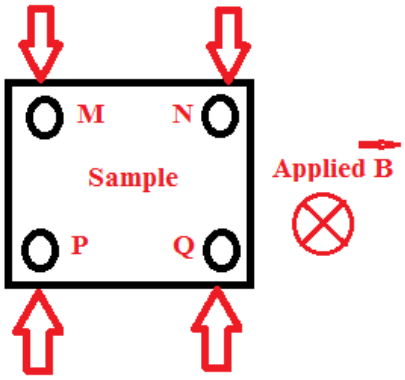

Fig. 4 – Schematic image of Hall Effect measurement system

The films were resistive (~ 10 kohms·cm) and the mobility of charge carrier ranged from 2 to 5 cm² /Vs as a result of Fe content in ZnO films.

4. CONCLUSIONS

Fe-doped ZnO film was successfully fabricated by the dip coating route. The X-rays diffraction confirmed the presence of the ZnO wurtzite structure. A (002)-oriented wurtzite crystal structure of ZnO doped with iron was confirmed by X-rays pattern. The grain size determined by X-rays diffraction was estimated between 25 and 35 nm. This nanoscale of grains was also estimated by SEM observation. High transmittance in visible and NIR spectra was detected. Although, p-type ZnO is instable phase, many researchers continue to report on p-type ZnO behavior. This study gives an opportunity to deep the research in this kind of ZnO conductivity.

Table 2 – Transmittance at 550 nm, optical band gap, bulk density, and mobility, resistivity and average Hall coefficient

Fe-Doping level (%)	T (550 nm) (%)	E_g (eV)	N_b ($10^{13} \times \mathrm{cm}^{-3}$)	μ (cm² / Vs)	ρ (10 kΩ·cm)	R_H ($10^5 \times \mathrm{cm}^3$/C)
2	83.8	3.24	2.07	5.540	5.43	3.01
3	81.44	3.26	4.07	2.523	6.07	1.53

ACKNOWLEDGMENTS

This study is included in the PNR project under contract number 8/U311/R77, supported by ATRST agency, http://www.atrst.dz, DG-RSDT NASR administration http://www.nasr.dz, and UST0-MB http://www.univ-usto.dz. The first author would like to thank the principal and all staff of central laboratory at DICLE University Diyarbakir Turkey for all efforts to achieve this work. I also thank the head of the microscope laboratory Pr. Hamzaoui S., USTO-Oran Algeria, for his help in performing the dip coating route. This is also a part of CNEPRU N° D01920120039, supported by the ministry of high teaching and scientific research http://www.mesrs.dz.

REFERENCES

1. M. Benhaliliba, C.E. Benouis, M.S. Aida, A. Sanchez Juarez, F. Yakuphanoglu, A. Tiburcio Silver, *J. Alloy. Compd.* **506**, 548 (2010).
2. M. Benhaliliba, C.E. Benouis, M.S. Aida, F. Yakuphanoglu, A. Sanchez Juarez, *J. Sol-Gel Sci. Technol.* **55**, 335 (2010).
3. C.E. Benouis, M. Benhaliliba, A. Sanchez Juarez, M.S. Aida, F. Chami, F. Yakuphanoglu, *J. Alloy. Compd.* **490**, 62 (2010).
4. P. Jongnavakit, P. Amornpitoksuk, S. Suwanboon, N. Ndiege, *Appl. Surf. Sci.* **258**, 8192 (2010).
5. Jian-Hui Sun, Shu-Ying Dong, Jing-Lan Feng, Xiao-Jing Yin, Xiao-Chuan Zhao, *J. Mol. Catal. A: Chem.* **335**, 145 (2011).
6. Cuong Ton-That, Matthew Foley, Laurent Lee Cheong Lem, Geoff Mc Credie, Matthew R. Phillips, Bruce C.C. Cowie, *Mater. Lett.* **64**, 386 (2010).
7. M.D. Carvalho, L.P. Ferreira, R.P. Borges, M. Godinho, *J. Solid State Chem.* **185**, 160 (2012).
8. Y.H. Xue, X.D. Zhang, X.L. Zhang, Y.Y. Shen, F. Zhua, L.H. Zhanga, J. Wanga, C.L. Liu, *Appl. Surf. Sci.* **257**, 10329 (2011).
9. Q.H. Luo, Y.H. Lu, Y.Z. Lou, Y.B. Wang, D.L. Yu, *Thin Solid Films* **518**, 7038 (2010).
10. H. Colak, O. Turkoglu, *J. Mater. Sci. Technol.* **28**, 268 (2012).